

ALICJA SZMIGIEL <sup>1\*</sup>, KRZYSZTOF TAJDUŚ <sup>2</sup>**A COMPREHENSIVE REVIEW OF SINKHOLE MODELING AND PREDICTION METHODS**

This article presents a comprehensive overview of the problem of sinkholes in mining and post-mining areas. It analyzes the key causes and mechanisms behind sinkhole formation, taking into account both natural factors and those resulting from human activity. Special attention is given to modeling methods and risk forecasting of sinkhole occurrence, based on a review of current scientific literature and the latest technological advancements, including advanced analytical techniques, numerical modeling and machine learning methods. The aim of this study is to expand both theoretical and practical understanding of sinkhole processes and to support the development of effective risk management strategies in regions affected by intensive mining activities.

**Keywords:** FEM; mining; rock mass; Machine Learning; Sinkholes

## 1. Introduction

Sinkholes are among the most significant geomechanical and geotechnical hazards, manifesting as a disruption of ground continuity and the sudden collapse of the land surface. These phenomena occurs both naturally and as a result of human activity (anthropogenic sinkholes). Natural causes are primarily associated with the presence of carbonate rocks such as limestone and dolomite, which are highly susceptible to karstification processes. Over time, these rocks gradually dissolve due to chemical interactions with groundwater, leading to the formation of underground voids and cavities. As these cavities expand and weaken the overlying material, the ground becomes increasingly unstable, making it more prone to sudden collapse [1]. Triggering factors are often linked to groundwater circulation, which causes erosion in the sediments above

<sup>1</sup> STRATA MECHANICS RESEARCH INSTITUTE POLISH ACADEMY OF SCIENCES, 27 REYMONTA STR., 30-059 KRAKÓW, POLAND

<sup>2</sup> AGH UNIVERSITY OF KRAKOW, AL. MICKIEWICZA 30, 30-059 KRAKÓW, POLAND

\* Corresponding author: [szmigiel.alicja@gmail.com](mailto:szmigiel.alicja@gmail.com)



© 2025. The Author(s). This is an open-access article distributed under the terms of the Creative Commons Attribution License (CC-BY 4.0). The Journal license is: <https://creativecommons.org/licenses/by/4.0/deed.en>. This license allows others to distribute, remix, modify, and build upon the author's work, even commercially, as long as the original work is attributed to the author.

cavity-bearing layers. For instance, fluctuations in the phreatic level due to pumping can intensify the local hydraulic gradient, while rainfall contributes to erosion both during infiltration and by sustaining underground water flows [2].

Anthropogenic sinkholes, on the other hand, are formed as a result of intensive underground extraction of mineral resources, which leads to significant disruption of the original structure of the rock mass, disturbances in hydrogeological conditions, and serious changes in the stress and strain state within the rock mass. A key factor predisposing the formation of sinkholes is the presence of shallow underground excavations. Over time, and under the influence of changing boundary conditions, these excavations lose stability, leading to the collapse of the overlying rock layers. As a result, the void created by the collapse of rocks into the excavation gradually migrates toward the surface, causing successive collapses of the higher-lying layers. The emergence of discontinuous surface deformation depends on specific geometric conditions. If the height of the collapse zone  $h_z$  reaches or exceeds the depth of the excavation  $H$ , or in the case of loose overburden layers at the surface, exceeds the difference between the excavation depth and the thickness of the loose overburden, discontinuous surface deformations will appear. Furthermore, if the combined height of the collapse zone and the fracture zone ( $h_z + h_s$ )  $\geq H$ , the resulting discontinuous deformations may be both surface-related and linear in nature. The type of deformation that forms depends on the size of the underground excavation as well as the type, physical-mechanical properties, and thickness of the soil layers overlying the excavation.

The causes of anthropogenic sinkhole formation are diverse, but they are always associated with shallow mining operations. The most significant triggering factors include:

- conducting mining operations at shallow depths or in fault zones with outcrops located close to the surface,
- collapse of old, shallow gallery excavations,
- activation of old, unsealed or improperly sealed mining shafts and winzes,
- overlapping edges of mining operations carried out simultaneously in multiple seams,
- fires in remnants of seams located at shallow depths,
- activation of secondary voids in the rock mass formed as a result of suffusion processes and other related phenomena.

The factors listed above are among the main causes of sinkhole formation; however, it is also important to consider the conditions that significantly accelerate the development of sinkhole processes, referred to as predisposing factors. These are primarily related to changes in soil and groundwater conditions, such as:

- the rise of mine water levels in areas of flooded mines, which leads to changes in the stress state of the rock mass and a decrease in the strength of rocks surrounding shallow underground workings,
- heavy rainfall leading to changes in rock properties and an increase in pore pressure, which can ultimately result in collapse and the formation of a sinkhole,
- active subsurface erosion caused by concentrated water inflow, which washes out material and alters the properties of rocks/soil in the immediate vicinity of underground workings.

The scientific literature presents numerous examples of sinkholes forming above or near active and abandoned mining sites [3-12]. Additionally, sinkholes can develop when loose fill soils or rock masses are disrupted by other human activities, such as metro or pipeline construction [13-16]. Some also form due to changes in natural water-drainage patterns and the introduction of

artificial water diversion systems such as water pumping stations. Furthermore failures in water supply infrastructure can cause uncontrolled water leakage into the subsoil and consequently accelerate subsurface erosion [2,4,17-20]

Sinkholes pose a significant threat to human life, infrastructure, and various activities, particularly in areas prone to their formation, as they can emerge suddenly and cause severe damage. The fact that sinkholes originate underground and often appear without warning makes risk mitigation and urban planning especially challenging. Predicting the exact timing and location of a sinkhole remains extremely difficult. Although certain factors can increase the likelihood of sinkhole formation to varying degrees, providing an early warning for an imminent collapse remains a complex task [21,22].

## 2. Initial observations on the impact of various factors on sinkhole formation

Observations conducted in two mining regions in Poland [23] showed that the majority of recorded sinkholes occurred where the overburden thickness ranged between 0 and 25 meters. The influence of overburden thickness on the number of sinkholes ( $n_1$ ) was described using the following function:

$$n_1 = 17.05 \cdot \exp(-0.012h_n) \quad (1)$$

where:  $h_n$  – thickness of loose overburden, m.

Whereas formula 2 illustrates the correlation between the thickness of the soil layers and the diameter of the sinkholes ( $d_1$ ):

$$d_1 = 2.53 \cdot h_n^{0.27} \quad (2)$$

As the thickness of the loose overburden increases, the probability of sinkhole occurrence decreases. When the overburden thickness is between 25 m and 70 m, sinkholes may occur occasionally; however, their diameters tend to increase (up to the critical thickness of 70 m). This increase is explained by the internal friction angle of the soil and the presence of quicksand layers within thicker overburden.

Similar statistical relationships were developed by Chudek Arkuszewski and Olaszowski [24] based on a large number of recorded and selected sinkholes. Their findings show that as many as 91.2% of sinkholes occur for workings located at depths ranging from 4 to 70 meters.

In 1980, Hunt [25] presented a diagram illustrating the conditions for the formation of sinkholes and continuous deformation, depending on the depth of the void and the ratio of the thickness of soil layers ( $h_n$ ) to the total overburden thickness ( $H$ ) (Fig. 1). As shown in the diagram, sinkholes formed under conditions where the initial depth of the collapsed mining excavations did not exceed 50 meters, and the ( $h_n/H$ ) ratio ranged from 0.1 to 1.1. Another study conducted in the South-Eastern mining region of Kotma [26] found that sinkholes primarily occurred for underground excavation depths up to 35 meters, with an ( $h_n/H$ ) ratio between 0.15 and 0.30. The likelihood of sinkhole formation decreases with an increasing ( $h_n/H$ ) ratio.

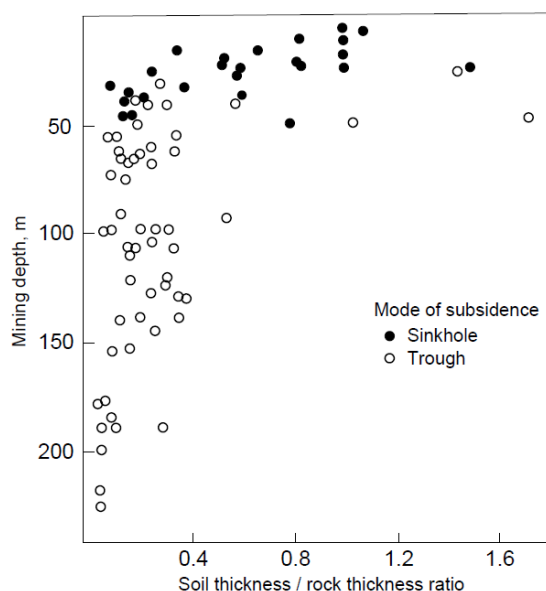


Fig. 1. The relationship between the ratio of soil thickness to the thickness of overburden rock depending on the depth of the excavation [25]

Matheson and Eckert-Clift [27] assumed that if the ratio of overburden thickness to the height of the underground excavation ( $g$ ) is less than 5, there is a high probability of sinkhole occurrence. Whereas, Statham and Treharne [28] demonstrated that 90% of all sinkholes occur when  $(H/g) < 6$ .

The presented studies on the critical values of the  $h_n/H$  and  $H/g$  ratios show significant discrepancies. These are related to differences in the test sites, which vary in terms of the depths of underground excavations, as well as in geological, soil, and hydrogeological conditions.

### 3. Sinkhole modeling methods

Predicting sinkhole formation requires advanced modeling approaches that can capture the complex geological, hydrological, and geotechnical factors involved. Various modeling methods have been proposed in the literature, ranging from empirical approaches based on observed relationships, to numerical models that simulate subsurface processes, and machine learning techniques that handle large datasets to identify patterns and predict future occurrences. Each of these methods has its own advantages and limitations, depending on data availability, computational requirements, and the specific characteristics of the study area.

#### 3.1. Empirical and analytical methods

Empirical methods allow for a relatively simple representation of the relationships between selected indicators that form the basis for assessing the likelihood of sinkhole occurrence on

the ground surface. This approach is based on the assumption that the carboniferous rock mass, in which the analyzed excavation is located, is characterized by constant values of bulk density and Poisson's ratio, as well as low tensile strength of the surrounding rocks. Additionally, it is assumed that the Carboniferous rock is overlain by a homogeneous layer of loose overburden (soil), which is characterized by a constant internal friction angle. As a result of the collapse of the void formed in the rock mass directly above the caved mining excavation and at a certain height above it, a collapse zone develops, consisting of displaced and detached rock blocks. If the depth of the excavation is sufficient, a fracture zone also forms above the collapse zone, where the rocks are intersected by numerous horizontal and lateral cracks. The issue of determining the height of these zones has been the subject of intensive scientific research for decades, dating back to the early 20th century (e.g., the work of Bierbaumer, [29]). Over the years, empirical formulas have been repeatedly modified depending on the mining exploitation method used or the quality of the rock mass. A summary of these relationships is presented, among others, in the work of Tajduś [30]. However, the approaches presented to date mainly refer to areas of large-scale mining operations, not to individual, isolated excavations such as drifts or their intersections.

The issue of the loss of stability in drift excavations has been the subject of detailed analytical studies conducted by accomplished researchers such as Cymbariewicz, Protodiakonov, Sałustowicz or Terzaghi. They attempted to provide a theoretical description of the destruction zone surrounding underground drifts, allowing for an approximate determination of their height and shape. The results of their studies are presented in detail in the publication by Tajduś et al. [31]. However, these approaches also did not account for the impact of the lithological variations of the overburden or the geometry of the excavation on the mechanism of sinkhole formation. These aspects were partially considered by other authors who – by introducing certain simplifications – undertook analytical attempts to estimate the probability of sinkhole occurrence at the surface.

In 1974, the Sachs-Zakolski-Skinderowicz [32] method was introduced. This approach is initially based on the Cymbariewicz method, which defines the so-called 'extend of void movement towards the surface of compacted layers', and subsequently calculates the radius of the unsupported portion of the roof of the compacted formations (Fig. 2):

$$r_p = R_p \sqrt{\frac{\ln \frac{a}{z - h_n}}{\ln \frac{a}{R_p}}} \quad (3)$$

where:

- $r_p$  – radius of the unsupported part of the roof in compacted rocks,
- $R_p$  – radius of the primary void (spherical in shape) representing the advancing void,
- $h_n$  – thickness of the unconsolidated overburden,
- $a$  – vertical extent of void propagation, determined using the formula:

$$a = \frac{2R_p}{1 + 2 \tan \left( 45^\circ - \frac{\varphi}{2} \right)} \cdot \frac{1}{1 - \frac{\sqrt{\mu \cdot \pi}}{2}} \quad (4)$$

where:

- $\mu$  – rock cohesiveness index,  
 $\varphi$  – internal friction angle of the collapsing rocks.

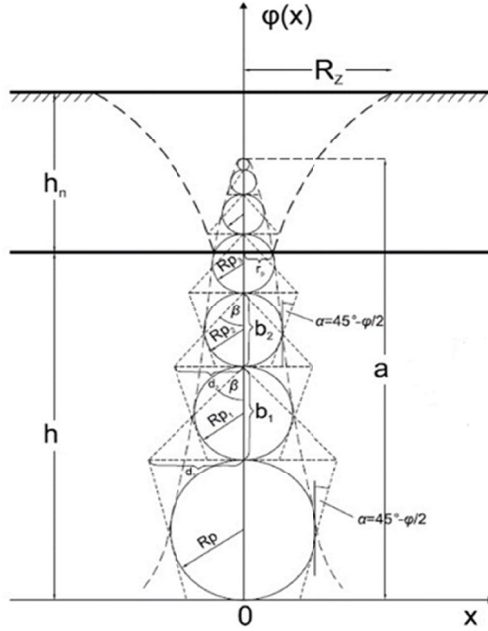


Fig. 2. Sinkhole formation model by Sachs, Skinderowicz, and Zakolski [32]

The function describing a sinkhole in consolidated formations takes the form of a bell-shaped curve (Fig. 2) and can be defined by the following formula:

$$\varphi(x) = 2R_p \frac{\sqrt{\mu}}{\sqrt{\mu} - 1.23} \exp \left[ - \left( \frac{x}{R_p} \right)^2 \ln \frac{2\sqrt{\mu}}{\sqrt{\mu} - 1.23} \right] \quad (5)$$

Another method for calculating the sinkhole process was presented by Janusz & Jarosz [33]. This model is based on the pressure arch theory, assuming that the tensile strength of rocks in the rock mass is close to zero. This assumption leads to the formation of a zone of relaxed rock in the shape of an ellipse above the void, where the rock material fractures, loosens, and falls to the bottom, forming an accumulated debris. The pressure arch supports the overlying rocks within the zone of initial stresses. A secondary void forms above the collapse, and the arch above it takes a shape similar to an elliptical dome. Assuming the horizontal semi-axes are equal, the ellipsoid becomes a rotational ellipsoid with a vertical axis  $c$  and a vertical semi-axis equal to  $L/2$ . The ratio of these axes remains constant under the given conditions:

$$n = \frac{c}{a} = 2 \frac{c}{L} \quad (6)$$

The value of  $n$  depends on the properties and condition of the rock mass:

- for compacted rocks ( $R_r > 0$ ):

$$n = \frac{p_z(1-2\nu) + R_r(1-\nu)}{2\nu} \quad (7)$$

- for rocks with very low tensile strength, ( $R_r \cong 0$ ):

$$n = \frac{1-2\nu}{2\nu} \quad (8)$$

- for heavily fractured rocks. ( $R_r = 0$ ):

$$n = \frac{1-\nu}{\nu} \quad (9)$$

where:  $\nu$  – poisson's ratio of the rocks in the caving zone

It is assumed that with an increase in the width of the void, the height of the pressure arch and the height of the collapse deposit increase, which leads to the formation of secondary voids. The volume of the secondary void can be calculated using a formula derived from the rock mass balance, which, after transformation, takes the following form:

$$V_p = L_d^2 g - (k_r - 1) \frac{\pi}{3n^2} \left[ P(z_2) - P\left(\frac{g}{2}\right) \right] \quad (10)$$

where:

- $g$  – height of the excavation,
- $L_d$  – length of the excavation,
- $k_r$  – rock loosening coefficient in the caving zone,
- $h$  – thickness of the compact rock layers above the void.

$$P(z_2) = 3c^2 z_2 - z_2^3; \quad z_2 = h + \left(\frac{g}{2}\right); \quad \text{for } c \geq h + \left(\frac{g}{2}\right)$$

$$P\left(\frac{g}{2}\right) = 3c^2 \left(\frac{g}{2}\right) - \left(\frac{g}{2}\right)^3; \quad z_2 = c; \quad \text{for } c < h + \left(\frac{g}{2}\right)$$

In the above formula, a crucial but difficult to determine parameter is the loosening coefficient  $k_r$ . The value of this coefficient, as determined by various researchers, is presented in the work of Tajduś [30]. However, since this coefficient depends on many factors such as moisture content, grain size, overburden pressure, and the physico-mechanical and chemical properties of the rocks, it is recommended – when assessing the possibility of sinkhole occurrence – to adopt a “worst-case” value that approximately accounts for the consolidation process of rocks in the collapse debris. It should be noted that, according to Staron's study [34], the rock loosening coefficient also depends on the compaction time, and there is a likelihood that, with sufficiently prolonged pressure, the value of  $k_r \approx 1.0$ .

Sachs [35,36] provided a formula for determining the critical depth of mine workings (measured from the roof of the excavation), for which a sinkhole will not form on the surface:

- for a drift excavation

$$H_{kr} = h_n + R_p \frac{2\sqrt{\mu}}{0.81\sqrt{\mu}-1} \cdot \sqrt{\frac{\mu}{\pi} \left( g \cdot L_d + \frac{L_d^2}{2\mu} \right)} \quad (11)$$

- for a post-exploitation void

$$H_{kr} = h_n + \frac{1.66\mu-1}{1.66\mu-2} \cdot \frac{g \cdot \sqrt{\mu}}{0.81\sqrt{\mu}-1} \quad (12)$$

where:

$H$  – depth of the excavation roof,

$\mu$  – Protodiakonov rock strength coefficient.

Another researcher who attempted to assess the possibility of sinkhole formation was Fenk [37]. Based on observations of discontinuous deformations, he determined the probability of sinkhole occurrence in unconsolidated rock mass above old lignite mine goafs and drifts within those goafs:

$$P = \exp \left\{ - \left[ 0.08(H-15) + 0.20h_b + 0.17h_n^{\max} \right] \right\} \quad (13)$$

where:

$P$  – probability of sinkhole occurrence,

$h_b$  – thickness of the immediate roof,

$h_n^{\max}$  – thickness of the thickest solid layer in the unconsolidated rock mass.

Chudek et al. [24] adopted the principle that the probability of discontinuous surface deformation depends on the value of the  $z$ -index, which defines the ratio of the depth of the collapsed excavation relative to the roof of the compacted rock mass to the height of the excavation ( $g$ ):

$$z = \frac{H - h_n}{g} \quad (14)$$

In 1996, Goszcz [38], based on the theory of ‘arch pressure,’ developed a model of the sinkhole formation process related to a void migrating towards the ground surface until complete self-filling occurs. In his assumptions, the author considered that the volume of the rock mass subject to collapse takes the shape of a pyramid with a square base, and that the rock mass in the collapse zone increases in volume by a loosening factor ( $k_r$ ). By adopting simplifications – namely, the horizontal excavation alignment and assuming the angle of collapse infill into the excavation equals the internal friction angle ( $\varphi$ ) – a simple relationship is obtained to determine the height of the void’s span:

$$h_z = \frac{3(g^2 \cot \varphi + g \cdot L)}{L(k_r - 1)} \quad (15)$$

It should be noted that Goszcz’s assumption of a pyramidal shape for the collapse zone is incorrect. Moreover, the weathering process in the upper part of the pyramid is less intense,



and there is also an additional effect of rock fragment wedging. This means that the actual height of the secondary void in the rock mass should be smaller than the one calculated using the formulas above.

In the work Subsidence: Occurrence, Prediction and Control, the authors Whittaker and Reddish [39], assuming a uniform rock density and minor changes in the bulk modulus of the fragmented rock ( $V_c$ ) in the collapse zone resulting from the increasing load on the rock fragments, defined a relationship for the volume of rock affected by the collapse (16).

$$V_c = \frac{1}{4} k_r h_z \pi D^2 \quad (16)$$

where:  $D$  – diameter of the void, m.

Then, by comparing the volume of the rock mass affected by the collapse with the volume of empty space in the excavation filled with the collapse debris, the authors presented a formula for the radius of the sinkhole at the ground surface:

$$R_z = \sqrt{\frac{L \cdot g \cdot (2g \cdot \cot \alpha_z + L)}{\pi \cdot h_z (k-1)}} \quad (17)$$

where:  $\alpha_z$  – Slope angle of the collapse debris in the excavation (angle of repose of collapsed rocks).

Based on studies conducted by Whittaker and Reddish [39], sinkholes tend to form within a period of 3 to 10 years after the collapse occurs above the intersection of underground excavations. However, both Polish and German experiences indicate that this period can be significantly longer – reaching up to 70 or even, in some cases, 100 years after finishing mining operations in shallow workings. Changes in hydrogeological conditions can significantly shorten this time and greatly intensify the sinkhole formation process [5].

In 2014, as a result of work conducted by researchers at IMG PAN [40], a series of models was developed to estimate the size of sinkholes on the ground surface for various configurations of underground mine workings. The starting point was the method proposed by Whittaker and Reddish [39]. Assuming a loss of stability of the underground excavation, the volume of the primary void responsible for sinkhole formation was calculated for four basic configurations of excavations (where  $\omega = g/l$ ):

- For the full intersection of two perpendicular excavations:  $V_p = \omega(2g \cot \alpha + L)$ ,
- For a partial intersection:  $V_p = \omega \left( \frac{3}{2} g \cot \alpha + L \right)$ ,
- For a longitudinal excavation:  $V_p = \omega(g \cot \alpha + L)$ ,
- For a dead-end excavation:  $V_p = \omega \left( \frac{1}{2} g \cot \alpha + L \right)$ .

The formulas presented above can be modified and adapted to any layout of mine workings. For example, for an assumed arrangement of excavations (Fig. 3) and assuming that the radius of the sinkhole ( $R_z$ ) is equal to the radius of the collapse cylinder in the rock mass ( $R$ ), the formula takes the following approximate form:

$$V_p \cong 2g^2 L \cot \alpha + gL^2 + 4\left(R - \frac{L}{2}\right)Lg \quad (18)$$

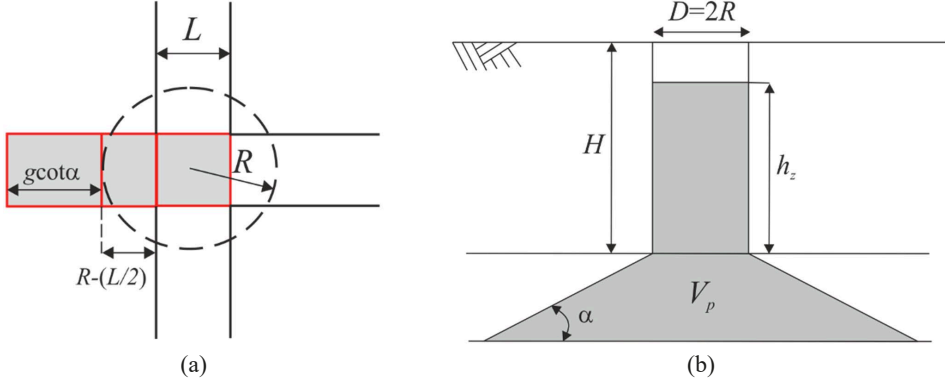


Fig. 3. Modified method for calculating the volume of the primary void causing sinkhole formation [40]

From the volume balance condition, a formula is derived for the height of the collapse necessary to completely fill the volume  $V_p$  and the cylindrical volume with height  $h_z$  in a loosened state:

$$h_z = \frac{V_p}{\pi R^2 (k_r - 1)} \quad (19)$$

In the case of a collapse occurring at a full intersection of excavations (assuming  $R = \frac{L}{2}$ ) the value obtained is:

$$h_z = \frac{4g}{\pi(k_r - 1)} \cdot \left(2 \frac{g}{L} \cot \alpha + 1\right) \quad (20)$$

As mentioned in the previous chapter, the occurrence of a sinkhole on the surface is possible when condition  $h_z \geq H$  or  $h_z \geq \frac{H}{SF}$  is met (SF – safety factor, which in global literature is commonly suggested to be of 1.3, however Tajduś and Sroka [41] are recommending adopting a value of 1.65). By applying the above methods and from the equilibrium condition, it is possible to determine the maximum depth of the sinkhole (in the case where the condition  $h_z \geq H$  is met).

$$S_z = \frac{4g}{\pi} \left(2 \frac{g}{L} \cot \alpha + 1\right) - (k_r - 1)H \quad (21)$$

It is important to remember that when determining the sinkhole depth ( $S_z$ ), the value of the rock loosening factor  $k_r$  decreases as a result of re-consolidation, which leads to an increase in the sinkhole depth.

The presented solution [42] applies only to “chimney-type” sinkholes and does not account for the further process of losing slope stability. Additionally, the  $k_r$  value refers to the entire

collapse process, which in reality is related to the geological structure of the analyzed area and may progress through both rock layers and soil layers. Therefore, for individual cases, the ratio  $h_n/H$  should be determined, and based on this ratio, the post-reconsolidation value of the factor should be adjusted accordingly.

### 3.2. Numerical modeling

Numerical modeling is a computational technique used to simulate physical phenomena by solving mathematical equations that describe their behavior. It works by discretizing a system into smaller elements or grids, applying governing equations (e.g., stress-strain relationships, fluid flow), and using iterative calculations to predict how the system evolves under various conditions. It has been widely used to analyze sinkhole formation and cavity stability across various geological settings, employing diverse computational approaches to capture different failure mechanisms.

Scientific literature provides several examples of numerical modeling applied to sinkhole formation, helping to analyze soil behavior, stress redistribution, and groundwater effects. Augarde et al. [43] explored the stability of submerged cavities using finite-element limit analysis, providing improved load parameter estimates compared to analytical solutions. It highlights the effectiveness of numerical methods in refining cavity collapse predictions under undrained conditions. Similarly, Shiau and Hassan [44], applied the shear strength reduction method (SSRM) using FLAC software to study sinkhole failure mechanisms in clay-rich soils, demonstrating strong soil arching effects and variations in surface failure extent depending on cavity geometry. Both studies emphasize the importance of failure mode analysis and load-bearing capacity assessment in predicting collapse events.

Scotto Di Santolo et al. [12] investigated sinkhole formation in the mining-affected hinterland of Naples, Italy, combining parametric analysis, borehole data, and numerical modeling with FLAC 2D. The study identified key stability factors, including rock strength, water infiltration, and cave geometry, revealing that elevated moisture levels significantly reduce structural integrity. The findings underscore the necessity of integrating hydrogeological factors into stability assessments. A concept also reflected in study conducted by Luu et al. [45], which applies a coupled hydromechanical model (LBM-DEM) to simulate the role of flooding in triggering collapses. This research differentiates between dropout and subsidence sinkholes, identifying erosion regimes influenced by hydraulic pressure and soil cohesion, ultimately demonstrating a linear relationship between collapse width and overlying soil height. These findings reinforce the significance of water-induced weakening as a critical precursor to sinkhole formation.

Sainsbury et al. [10] focused on large-scale mine subsidence modeling, using historical monitoring data to validate numerical simulations of cave propagation. The study confirms that hydraulic fracturing plays an important role in facilitating gravity-driven failure, with subsidence behavior strongly influenced by pre-existing fault structures. The results showcase the importance of back-analysis techniques for calibrating numerical models and optimizing predictive accuracy, a concept also explored by Baric and Kovacevic Zelic [46]. This study examines earthquake-induced sinkholes in Croatia using PLAXIS 2D and FLAC simulations, showing that soil strength and cavity shape significantly impact failure modes. Notably, non-circular caverns experience higher vertical displacements due to altered stress distributions, while brittle clays are more prone to tension cut-off failure. Another study from the Ghor Al-Haditha sinkhole site in Jordan reveals that weak interlayers accelerate failure, particularly in stratified deposits [47]

An integrated geophysical approach is presented by Ścigała et al. [8], which combines electrical resistivity tomography (ERT) with FLAC 3D modeling to assess sinkhole hazards in Poland's Upper Silesian Coal Basin. The study demonstrates that ERT effectively detects subsurface voids, while numerical modeling refines the assessment of potential collapse zones. This hybrid methodology enhances risk evaluation, suggesting that forward numerical modeling serves as a valuable complement to geophysical surveys. Across all of studies, a common limitation is the simplification of soil and rock behavior, with several [12,45,46] emphasizing the need for more advanced constitutive models that account for coupled volumetric deformation and strain-softening effects. Furthermore, the role of water table fluctuations, hydraulic forces, and multi-physics interactions remains a challenge in achieving fully predictive models.

Some studies compare numerical modeling with small-scale physical models to investigate sinkhole formation and soil behavior. Soliman et al. [48] examines cover-collapse sinkholes in Central Florida through physical and numerical methods. A small-scale physical model simulates cavity propagation due to a fracture at the boundary between two aquifers, showing an inverted triangular cavity growth until collapse. A numerical model replicates this shape to analyze stress redistribution, seepage forces, and stability under different groundwater conditions. Results highlight the role of soil arching, increased stress at cavity corners, and the influence of groundwater levels and cavity shape on stability. Caudron et al. [49] explored soil-structure interactions during sinkhole formation using a coupled numerical approach (FLAC2D and PFC2D) and validates it against a small-scale experimental model. The study finds that the numerical simulation better captures the overall settlement trough volume and predicts settlement and slope values more accurately than semi-empirical methods.

Overall, these studies underscore the growing reliance on numerical modeling techniques, from finite-element and finite-difference methods to discrete element and hydromechanical coupling approaches, in understanding sinkhole mechanisms. While numerical models provide essential insights into cavity stability and failure propagation, the integration of field data, laboratory testing, and advanced constitutive modeling remains critical for enhancing their predictive capabilities.

### **3.3. Machine Learning**

Machine learning is transforming engineering research by enabling data-driven insights and predictive modeling in complex geotechnical problems. In the context of sinkhole prediction, ML algorithms can analyze large amounts of data collected from various monitoring techniques, such as GPR, InSAR and in-situ sensors, to detect patterns and identify early warning signs of potential collapse. By learning from historical data, these models can improve prediction accuracy and provide risk assessments. Research literature includes several successful applications of machine learning in sinkhole prediction, demonstrating its effectiveness in analyzing geospatial and geotechnical data to identify high-risk areas.

#### **3.3.1. Classic Machine learning applications**

Several studies emphasize the importance of high-resolution LiDAR data in identifying potential sinkhole depressions. Zhu et al. [50] applied six machine learning models – logistic regression, naive Bayes, neural networks, random forests, RUSBoost, and support vector ma-

chines – on a dataset of 22,884 records, achieving strong classification performance with AUC values exceeding 0.87. The neural network model stood out, attaining an AUC of 0.95 and a testing accuracy of 85%. A novel two-step approach integrating machine learning predictions with manual visual inspection significantly reduced the need for exhaustive manual verification. Similarly, Zhu and Pierskalla [51] utilized a random forest classifier trained on LiDAR-extracted depressions in Kentucky, employing 11 morphometric and environmental variables to differentiate sinkholes from other depressions. A weighted approach improved classification accuracy to 89.95% in the training dataset, though performance declined to 73.96% when applied to a different geological setting, showing the limitations of model generalizability. A LiDAR-based machine learning approach have also been successfully applied in identifying sinkholes in in the Nixa Karst Plain in Missouri [52]. The study incorporated adaptive filtering, watershed segmentation, and a random forest classifier. Depth and area were found to be the most influential features, leading to 87.9% accuracy.

The integration of hydrogeological parameters has also been crucial for improving sinkhole susceptibility modeling. Kim et al. [53] developed a sinkhole hazard map for East Central Florida using an artificial neural network trained on seven hydrogeological variables, such as hydraulic head difference, groundwater recharge rate, and soil permeability. The study demonstrated that regions with thick overburden layers tend to produce larger sinkholes, aligning with known geological behaviors. In contrast, Taheri et al. [54] investigated sinkhole formation in Hamadan Province, Iran, using Bayesian classifiers (Bayes net, naive Bayes, Bayesian logistic regression) and logistic regression. The study incorporated ten conditioning factors, including groundwater exploitation, bedrock lithology, and fault density, ultimately finding that Bayesian models outperformed traditional statistical approaches in modeling complex, multi-factorial sinkhole susceptibility. Additionally, a study by Bianchini et al. [55] applied the MaxEnt (Maximum Entropy) machine learning model to assess sinkhole susceptibility and risk in the Guidonia-Bagni di Tivoli plain, Italy. Using eight environmental factors, including lithology, land use, groundwater levels, and InSAR-derived ground deformation data, the study identified lithology, travertine thickness, and fault proximity as the most influential contributors. The research further integrated geo-topographical cadastral records to produce a risk classification map, revealing that high-risk zones corresponded to urbanized areas with extensive groundwater extraction and structural loads.

Beyond topographic and hydrogeological data, remote sensing techniques such as InSAR have been explored for sinkhole monitoring followed by machine learning evaluation. Nefeslioglu et al. [56] combined InSAR-based deformation analysis with an artificial neural network to assess sinkhole susceptibility in Turkey, particularly in areas planned for high-speed railway construction. The model leveraged nine months of ground displacement data from Sentinel-1A and 1B satellites alongside six topographic parameters, revealing strong correlations between high-deformation zones and sinkhole-prone areas. This study shows the potential of integrating remote sensing data with machine learning models for large-scale, long-term sinkhole monitoring.

A common theme across these studies is the selection of influential predictive variables. While morphometric parameters such as depth, volume, and shape complexity [52] consistently rank as important, the inclusion of environmental and anthropogenic factors has enhanced model performance. For instance, Zhu and Pierskalla [51] identified land-use, berm slope, and bottom roughness as critical factors in sinkhole classification, while Taheri et al. [54] found that groundwater-related parameters such as water level decline and deep well penetration significantly contributed to susceptibility assessments. Similarly, Bianchini et al. [55] emphasized the

importance of land-use activities such as quarrying and urban expansion in sinkhole susceptibility, demonstrating that continuous urbanization can intensify collapse mechanisms due to increased structural loads and groundwater exploitation.

Despite their advancements, machine learning-based sinkhole models face limitations, primarily related to transferability and validation. Miao et al. [52] highlighted challenges in detecting embryonic sinkholes, as these features often lack well-defined topographic signatures. Some reported decreased accuracy when applying trained models to new regions with differing geological conditions, emphasizing the need for site-specific calibration [50,51]. Moreover, they acknowledged that machine learning cannot fully replace manual verification; instead, it should be used to prioritize areas for further investigation, thereby reducing time and labor costs. Likewise, the MaxEnt study in Italy [55] encountered challenges in integrating hydrogeological data, particularly due to incomplete records on groundwater wells and aquifer properties. The research further noted the limitations of InSAR in detecting rapid sinkhole formation events.

### 3.3.2. Deep Learning Models for sinkhole detection from images

Machine learning, and especially deep learning, has been widely explored in research for extracting information and detecting sinkholes from remote sensing images. Traditional methods rely on manually defined features, while deep learning approaches, such as convolutional neural networks (CNNs), automatically learn spatial patterns from image data. For instance, Alrabayah et al. [57] employed a U-Net model trained on high-resolution drone orthophotos and later fine-tuned using satellite imagery, achieving high recall (96.79% for drone images, 92.06% for satellite images). The transition from high-resolution local data to lower-resolution satellite imagery showcases the model's adaptability, although resolution differences introduce some precision loss. Similarly, Rafique et al. [58] applied a U-Net to segment sinkholes in digital elevation models (DEMs), finding that DEM gradient images with Gaussian normalization yield the highest accuracy, while aerial imagery alone is ineffective.

For subsurface sinkhole detection, GPR data has been processed using deep learning to enhance classification accuracy. Kang et al. [59] introduces UcNet, which integrates CNN-based classification with super-resolution (SR) image generation and phase analysis to refine cavity detection. The super-resolution step improves feature distinction, minimizing confusion with gravel, and ultimately reduces misclassification errors in urban environments. The importance of image preprocessing is also highlighted by Lee et al. [60] and Vu et al. [61], which focus on UAV-mounted thermal infrared (IR) imaging. Two-stage CNN system combines U-Net for semantic segmentation with MobileNet v3 for classification, tracking sinkholes in real-time with an IoU (intersection over union) of 88% [61]. Meanwhile, Lee et al. [60] employs an ensemble of CNN and Boosted Random Forest (BRF) classifiers, leveraging thermal anomaly patterns to improve detection accuracy. The study confirms that both CNN-extracted and handcrafted features contribute significantly to classification, particularly in varying environmental conditions.

Despite these advances, several limitations persist across these methods. The dependency on high-quality training data remains a challenge [57], where manual annotation introduces subjectivity. Vu et al. [61] acknowledge that real-world sinkholes exhibit greater variability than the artificial sinkholes used for training in their study. Additionally, resolution constraints in lower-quality satellite imagery [57] and unstable video input in UAV-based detection [61] impact accuracy. Lastly, factors influencing detection performance vary across modalities – DEM gradient

data proved essential in elevation-based models [58], while temperature contrast and seasonal effects influenced thermal imaging methods [60]. Despite these challenges, the integration of deep learning with diverse data sources continues to enhance sinkhole detection and monitoring, supporting more scalable and automated hazard assessment frameworks.

## 4. Discussion

In the presented approaches to forecasting sinkholes in post-mining areas, clear differences can be observed in their capabilities, scope of application, and limitations. These differences primarily stem from varying theoretical assumptions, the complexity of the models, and the requirements for data availability. Analytical methods, based on simplified geometries of collapse zones and homogeneous materials, are primarily used as preliminary assessment tools. Their greatest advantage lies in their relatively low computational demand and procedural transparency: an engineer can quickly estimate the potential sinkhole extent and its basic parameters using explicit equations and simple geometric-mechanical relationships. In practice, this means such methods can be applied in the early phases of design or site monitoring when only partial geotechnical data is available. On the other hand, the assumptions made in analytical models – such as isotropy and homogeneity of the rock-soil medium and the simplified shape of the collapse zone (e.g., conical or hemispherical) – limit their usefulness for precise predictions in complex geological conditions, where strong heterogeneity, stratification, anisotropy, and local irregularities of mining excavations occur.

Numerical methods, in contrast, allow for the inclusion of a wide range of physico-mechanical factors, such as various rock and soil layers, fractures, variability in water saturation, or nonlinear material behavior. Developing a model requires both a physical representation – selecting key parameters of the geological and mining structure – and a mathematical description, which involves choosing suitable brittle-plastic criteria (such as the Coulomb-Mohr theory or clay plasticity models) as well as parameters of elasticity or viscosity. Two-dimensional simulations found in the literature, typically based on elasto-plastic models, have shown that numerical methods allow tracking the initiation of the collapse zone, its propagation, and potential “chimneying” within the overburden. This enables the analysis of how changes in loading, excavation geometry, or hydrogeological conditions affect deformation development. However, in practice, applying these tools on a regional scale encounters significant difficulties. Firstly, the computational cost of three-dimensional analyses becomes very high, and the need for multiple simulation runs makes quick decision-making challenging. Secondly, the requirement for precise calibration of material parameters over large areas is nearly impossible to meet due to the natural heterogeneity and anisotropy of the rock mass – physico-mechanical tests conducted at one point often do not reflect conditions several dozen of meters away. Finally, the complexity of numerical models necessitates a compromise between detail and computational stability, requiring high expertise from engineering and geomechanics teams.

In recent years, growing interest has been placed in machine learning methods, which, thanks to advanced algorithms, can detect hidden relationships in large geotechnical and mining datasets. Neural networks, random forests, or support vector machines allow efficient processing of dozens or even hundreds of input variables – from rock strength parameters and excavation depth to geometry characteristics and exploitation history. After the training phase, these models can



promptly estimate the probability of sinkhole occurrence at any point in the study area, making them attractive tools for continuous monitoring and rapid response. However, the quality of such forecasts depends heavily on the availability of representative and well-structured datasets – gaps in geotechnical measurements, scattered laboratory samples, or inconsistent historical records can lead to inaccurate predictions and reduced prediction capability. Moreover, many ML algorithms operate as “black boxes” – although they provide accurate predictions, it is often difficult to determine which factors influenced the final decision and how, which limits their acceptance in engineering environments where transparency and verifiability are critical.

Considering the mentioned strengths and weaknesses, there is a growing need for the development of hybrid approaches that combine the advantages of several techniques. In practice, a well-structured hybrid workflow could begin with quick analytical assessments to define potentially hazardous areas based on simple geometric and mechanical assumptions. These initial results can assist in targeted data collection and the development of detailed numerical models. In the second stage, numerical modeling can simulate stress distribution and collapse propagation under various geological and hydrogeological conditions, providing potential scenarios for collapse zone development and synthetic datasets for difficult to monitor scenarios. These outputs, alongside historical and monitoring data, can then serve as training input for machine learning algorithms. The role of ML would be to generalize patterns learned from simulations and real-world cases, enabling predictions in areas where either numerical modeling is computationally infeasible or monitoring data is incomplete. Additionally, interpretability techniques like SHAP (SHapley Additive exPlanations) or LIME (Local Interpretable Model-Agnostic Explanations) can enhance trust in ML predictions, presenting insight into the contribution of individual features. Such a hybrid strategy could not only improve forecasting accuracy but also offers a framework to address some of the known gaps highlighted in individual modeling approaches. For instance, limitations in analytical and numerical methods – such as simplified constitutive assumptions or the challenge of modeling dynamic water table conditions – could be partially mitigated by integrating more flexible data-driven models. Such strategy provides a scalable framework adaptable to various geological and mining conditions.

In addition to the established methodologies discussed in this review, it is worth briefly noting the growing relevance of emerging technologies in the context of sinkhole prediction. Advances in deep learning, have shown great promise in recognizing complex spatial and temporal patterns from large and unstructured datasets. These methods could enable more accurate and automated forecasting models, especially when integrated with time-series data from long-term monitoring. Simultaneously, developments in advanced remote sensing techniques – such as high-resolution InSAR, hyperspectral imaging, and drone-based photogrammetry – offer increasingly detailed, spatially continuous information on ground deformation and subsurface changes. The integration of such methods into predictive workflows may significantly enhance early-warning capabilities and support more proactive risk mitigation strategies in post-mining areas.

## 5. Conclusion

The issue of forecasting the occurrence of sinkholes in post-mining areas is one of the most challenging problems in engineering geomechanics, combining the randomness of the process with complex geological and mining interactions. This article emphasizes that regardless of the chosen forecasting method – whether analytical, numerical, or based on machine learning – the



key factor is a thorough initial assessment of local conditions. In practice, this requires detailed mining investigations, supplemented by in situ analyses of the mechanical and hydrogeological properties of rocks and soils. Only on the basis of reliable data is it possible to properly adjust numerical models that account for heterogeneity, anisotropy, and the nonlinear behavior of rock material under the influence of underground mining.

The analyses show that analytical methods are highly effective in the initial phase of risk assessment, offering quick and transparent estimates of the collapse zone extent with minimal data requirements. However, their geometric simplifications and assumptions of medium homogeneity limit their accuracy under real-world conditions, where geological structures are often complex and irregular. Numerical simulations, on the other hand, enable modeling of the complex mechanisms behind the formation and development of collapse zones but require significant computational resources and precise parameters obtained from an extensive range of field and laboratory studies. Machine learning methods are gaining importance due to their ability to process large datasets and rapidly generate risk forecasts for many locations simultaneously. However, their effectiveness largely depends on the quality and integrity of the training datasets, and the “black box” nature of some algorithms raises concerns about transparency and interpretability of results in engineering contexts. The authors emphasize that no single approach provides a comprehensive solution. Each method should be seen as a complementary tool: analytical algorithms serve to preliminarily identify high-risk areas, numerical simulations provide detailed information on stress distribution and potential collapse mechanisms, and ML models – trained on data from simulations and field monitoring – enable rapid forecasting for new scenarios.

Moreover, the systematic development and unification of geotechnical and mining databases, as well as the implementation of long-term field monitoring programs, are of utmost importance. Such an approach will not only support the continuous improvement of algorithms and models but also enable real-world validation of forecasting accuracy. This, in turn, will facilitate the development of effective, reliable, and economically justified predictive tools adjusted to the diverse geological and mining conditions of post-mining areas.

## Acknowledgment

This research was funded by RESEARCH FUND FOR COAL AND STEEL (RFCS), grant number 101157400 and by the POLISH MINISTRY OF EDUCATION AND SCIENCE, grant number 5997/FBWiS/2024/2 (no W 109/FBWiS/2024) under the project SIRIMA “Sinkhole hazard and risk management in post-mining areas”. The authors gratefully acknowledge the funding provided.

## References

- [1] A.K. Abd El Aal, B.S. Nabawy, A. Aqeel, A. Abidi, Geohazards assessment of the karstified limestone cliffs for safe urban constructions, Sohag, West Nile Valley, Egypt. *Journal of African Earth Sciences* **161**, 103671 (2020). DOI: <https://doi.org/10.1016/j.jafrearsci.2019.103671>
- [2] E. Intrieri, G. Gigli, M. Nocentini, L. Lombardi, F. Mugnai, F. Fidolini, N. Casagli, Sinkhole monitoring and early warning: An experimental and successful GB-InSAR application. *Geomorphology* **241**, 304-314, (2015). DOI: <https://doi.org/10.1016/j.geomorph.2015.04.018>
- [3] J.-W. Kim, Z. Lu, J. Kaufmann, Evolution of sinkholes over Wink, Texas, observed by high-resolution optical and SAR imagery. *Remote Sensing of Environment* **222**, 119-132 (2019). DOI: <https://doi.org/10.1016/j.rse.2018.12.028>

- [4] K. Konieczny, L. Słowik, An Example of Failure of an Office Building in Upper Silesia. *MATEC Web Conf* **284**, 3003 (2019). DOI: <https://doi.org/10.1051/mateconf/201928403003>
- [5] A. Kotyrba, Ł. Kortas, Sinkhole hazard assessment in the area of abandoned mining shaft basing on microgravity survey and modelling – Case study from the Upper Silesia Coal Basin in Poland, *Journal of Applied Geophysics* **130**, 62-70 (2016). DOI: <https://doi.org/10.1016/j.jappgeo.2016.04.007>
- [6] A.A. Malinowska, A. Guzy, R. Hejmanowski, P. Ulmaniec, Hybrid-approach for sinkhole occurrence risk mitigation in urban areas. *IOP Conf. Ser.: Earth Environ. Sci.* **291**, 12022 (2019). DOI: <https://doi.org/10.1088/1755-1315/291/1/012022>
- [7] A.A. Malinowska, A. Matonóg, Sinkhole hazard mapping with the use of Spatial analysis and analytical hierarchy process in the light of mining-geological factors. *Acta Geodynamica et Geomaterialia* **14**, 2 (186), 159-172 (2016). DOI: <https://doi.org/10.13168/AGG.2016.0037>
- [8] R. Ściagała, K. Szafulera, M. Jendryś, Assessment of sinkhole hazard in the post-mining area using the ERT method and numerical modeling. *75 Scientific Journals of the Maritime University of Szczecin* **147**, 20-34 (2023). DOI: <https://doi.org/10.17402/570>
- [9] P. Sahu, R.D. Lokhande, An Investigation of Sinkhole Subsidence and its Preventive Measures in Underground Coal Mining. *Procedia Earth and Planetary Science* **11**, 63-75 (2015). DOI: <https://doi.org/10.1016/j.proeps.2015.06.009>
- [10] B.-A. Sainsbury, D. Sainsbury, D. Carroll, Back-analysis of PC1 cave propagation and subsidence behaviour at the Cadia East mine. *Proceedings of the Fourth International Symposium on Block and Sublevel Caving*, Australian Centre for Geomechanics, 167-78 (2018) DOI: [https://doi.org/10.36487/ACG\\_rep/1815\\_10\\_Sainsbury](https://doi.org/10.36487/ACG_rep/1815_10_Sainsbury)
- [11] T. Sasaoka, H. Takamoto, H. Shimada, J. Oya, A. Hamanaka, K. Matsui, Surface subsidence due to underground mining operation under weak geological condition in Indonesia. *Journal of Rock Mechanics and Geotechnical Engineering* **7**, 337-344 (2015). DOI: <https://doi.org/10.1016/j.jrmge.2015.01.007>
- [12] A. Scotto Di Santolo, G. Forte, A. Santo, Analysis of sinkhole triggering mechanisms in the hinterland of Naples (southern Italy). *Engineering Geology* **237**, 42-52 (2018). DOI: <https://doi.org/10.1016/j.enggeo.2018.02.014>
- [13] X. Chen, Y. Hu, L. Zhang, Y. Liu, 3D large-deformation modelling on face instability and sinkhole formation during tunnelling through non-uniform soils. *Tunnelling and Underground Space Technology* **134**, 105011 (2023). DOI: <https://doi.org/10.1016/j.tust.2023.105011>
- [14] Y. Hou, Q. Fang, D. Zhang, L.N.Y. Wong, Excavation failure due to pipeline damage during shallow tunnelling in soft ground. *Tunnelling and Underground Space Technology* **46**, 76-84 (2015). DOI: <https://doi.org/10.1016/j.tust.2014.11.004>
- [15] K. Zhang, W. Zheng, Z. Liao, H. Xie, C. Zhou, S. Chen, J. Zhu, Risk assessment of ground collapse along tunnels in karst terrain by using an improved extension evaluation method. *Tunnelling and Underground Space Technology* **129**, 104669 (2022). DOI: <https://doi.org/10.1016/j.tust.2022.104669>
- [16] Y. Zhang, Y.-Y. Jiao, L.-L. He, F. Tan, H.-M. Zhu, H.-L. Wei, Q.-B. Zhang, Susceptibility mapping and risk assessment of urban sinkholes based on grey system theory. *Tunnelling and Underground Space Technology* **152**, 105893 (2024). DOI: <https://doi.org/10.1016/j.tust.2024.105893>
- [17] H. Ali, J. Choi, Risk Prediction of Sinkhole Occurrence for Different Subsurface Soil Profiles due to Leakage from Underground Sewer and Water Pipelines. *Sustainability* **12**, 310 (2019). DOI: <https://doi.org/10.3390/su12010310>
- [18] M. Dave, A. Juneja, Erosion of soil around damaged buried water pipes – a critical review. *Arab. J. Geosci.* **16**, 317 (2023). DOI: <https://doi.org/10.1007/s12517-023-11391-4>
- [19] P.M. Guarino, A. Santo, G. Forte, M. De Falco, D.M.A. Niceforo, Analysis of a database for anthropogenic sinkhole triggering and zonation in the Naples hinterland (Southern Italy). *Nat Hazards* **91**, 173-192 (2017). DOI: <https://doi.org/10.1007/s11069-017-3054-5>
- [20] F. Sari, Sinkhole susceptibility analysis for karapınar/konya via multi criteria decision. *ISPRS Ann. Photogramm. Remote Sens. Spatial Inf. Sci.* **IV-4/W4**, 339-343 (2017). DOI: <https://doi.org/10.5194/isprs-annals-IV-4-W4-339-2017>
- [21] E. Intrieri, P. Confuorto, S. Bianchini, C. Rivolta, D. Leva, S. Gregolon, V. Buchignani, R. Fanti, Sinkhole risk mapping and early warning: the case of Camaiole (Italy). *Front Earth Sci.* **11**, 1172727 (2023). DOI: <https://doi.org/10.3389/feart.2023.1172727>

- [22] R.N. Nof, M. Abelson, E. Raz, Y. Magen, S. Atzori, S. Salvi, G. Baer, SAR Interferometry for Sinkhole Early Warning and Susceptibility Assessment along the Dead Sea. *Israel. Remote Sensing* **11**, 1, 89 (2019). DOI: <https://doi.org/10.3390/rs11010089>
- [23] E. Mikula, Tworzenie się deformacji zapadliskowych w luźnym nadkładzie jako przypowierzchniowej warstwie górotworu, *Ochrona Terenów Górniczych* **79/1**, 17–24 (1987).
- [24] M. Chudek, J. Arkuszewski, W. Olaszowski, Deformacje nieciągłe w obszarach górniczych, *Z. 101 = Nr 610*, Wydawnictwo Politechniki Śląskiej, 1980, Gliwice.
- [25] S.R. Hunt, Surface Subsidence due to Coal Mining in Illinois. PhD Thesis, University of Illinois at Urbana-Champaign, 1980.
- [26] K.B. Singh, B.B. Dhar, Sinkhole subsidence due to mining. *Geotechnical and Geological Engineering* **15**, 327-341 (1997). DOI: <https://doi.org/10.1007/BF00880712>
- [27] G.M. Matheson, A.D. Eckert-Clift, Characteristics of chimney subsidence and sinkhole development from abandoned underground coal mines along the Colorado Front Range. *Proceedings of the 2nd Workshop on Surface Subsidence Due to Underground Mining*, West Virginia University, Morgantown, 204-214, 1986.
- [28] I. Statham, G. Treharne, Subsidence due to abandoned mining in the South Wales Coalfield, U.K.: Causes, mechanisms and environmental risk assessment. *Proceeding of the Fourth International Symposium on Land Subsidence*, Houston, Texas 200, 143-152, 1991.
- [29] A. Bierbaumer, Die Dimensionierung des Tunnelmauerwerkes: Studien, Leipzig, Deutschland, Wilhelm Engelmann, 1923.
- [30] K. Tajduś, Determination of the Value of the Strain parameters for Strata Rock Mass in the Region of Underground Mining Influence. *VGE Verlag GmbH* 2 (2009).
- [31] A. Tajduś, K. Tajduś, M. Cała, *Geomechanika w budownictwie podziemnym. Projektowanie i budowa tuneli*. Wydawnictwo AGH, Kraków. 2012.
- [32] J. Sachs, B. Skinderowicz, R. Zakolski, Prognozowanie rodzaju i wielkości deformacji nieciągłych powierzchni na terenach płytkiej eksploatacji górniczej. *Mat. Konf. Nauk.-Techn. pt.: Wybrane zagadnienia budownictwa na terenach górniczych*, Katowice-Jaszowiec, 1974.
- [33] W. Janusz, A. Jarosz, Nieciągłe deformacje powierzchni terenu wywołane płytką podziemną eksploatacją górniczą. *Mat. Konf. Nauk.-Techn. pt.: Budownictwo na terenach o dużych deformacjach*, Katowice, 1976.
- [34] T. Staroń, Eksploatacja pokładów węgla z zawałem stropu w sąsiedztwie pól pożarowych. *W. Śląsk, Katowice*, (1979).
- [35] J. Sachs, Metoda prognozowania nieciągłych deformacji powierzchni ziemi na terenach górniczych. *Konferencja Naukowo Techniczna na temat „Problemy budownictwa na terenach zapadliskowych”*, Częstochowa, 1978.
- [36] J. Sachs, Prognozowanie powstawania zapadliska powierzchni ziemi na podstawie informacji wynikających z rozeznania geologiczno-górniczego badanego terenu. *Konferencja Naukowo Techniczna na temat „Problemy budownictwa na terenach zapadliskowych”*, Częstochowa, 1978.
- [37] J. Fenk, Eine Theorie zur Entstehung von Tagesbrüchen über Hohlräumen im Lockergestein. *Dissertation, unveröff, Bergakademie Freiberg*, 1979.
- [38] A. Goszcz, Powstawanie zapadlisk i innych deformacji nieciągłych powierzchni na obszarach płytkiej eksploatacji górniczej. *Mat. Konf. pt.: Szkoła Eksploatacji Podziemnej '96*, Wyd. CPPGSMiE PAN, 119-137, 1996.
- [39] B.N. Whittaker, D.J. Reddish, *Subsidence Occurrence, Prediction and Control*, **56**. Nottingham: ELSEVIER. 1989.
- [40] M. Clostermann, Einwirkungsrelevanz des Altbergbaus, Bemessung von Einwirkungs- und Gefährdungsbereichen und Einfluss von Grubenwasserstandsänderungen. *Gutachterliche Stellungnahme, Projekt Nr.: 16-124*, 2020.
- [41] K. Tajduś, A. Sroka, Analytic and numerical methods of sinkhole prognosis. *Altbergbau Kolloquium Verlag Glückauf GmbH, Freiberg*, 152-65 (2007).
- [42] A. Sroka, K. Tajduś, R. Misa, M. Clostermann, The possibility of discontinuity/sinkholes appearance with the determination of their geometry in the case of shallow drifts. *Prognose von Tagesbrüchen Und Deren Geometrie Bei Tagesnahen Strecken 18 Altbergbau – Kolloquium*, 173-86 (2018).
- [43] C.E. Augarde, A.V. Lyamin, S.W. Sloan, Prediction of Undrained Sinkhole Collapse. *J. Geotech. Geoenviron. Eng.* **129**, 197-205 (2003). DOI: [https://doi.org/10.1061/\(asce\)1090-0241\(2003\)129:3\(197\)](https://doi.org/10.1061/(asce)1090-0241(2003)129:3(197))

- [44] J. Shiau, M.M. Hassan, Numerical modelling of three-dimensional sinkhole stability using finite different method. *Innov Infrastruct Solut* **6**, 183 (2021). DOI: <https://doi.org/10.1007/s41062-021-00559-0>
- [45] L.-H. Luu, G. Noury, Z. Benseghier, P. Philippe, Hydro-mechanical modeling of sinkhole occurrence processes in covered karst terrains during a flood. *Eng. Geol.* **260**, 105249 (2019). DOI: <https://doi.org/10.1016/j.enggeo.2019.105249>
- [46] A. Baric, B. Kovacevic Zelic, Numerical modelling of cover-collapse sinkholes caused by the earthquake – a case study. *ISSMGE* (2022). DOI: <https://doi.org/10.53243/ICEG2023-263>
- [47] D. Al-Halbouni, E.P. Holohan, A. Taheri, M.P.J. Schöpfer, S. Emam, T. Dahm, Geomechanical modelling of sinkhole development using distinct elements: model verification for a single void space and application to the Dead Sea area. *Solid Earth* **9**, 1341-1373 (2018). DOI: <https://doi.org/10.5194/se-9-1341-2018>
- [48] M.H. Soliman, A.L. Perez, B.H. Nam, M. Ye, Physical and Numerical Analysis on the Mechanical Behavior of Cover-collapse Sinkholes in Central Florida. *Proceedings of the 15th Multidisciplinary Conference on Sinkholes and the Engineering and Environmental Impacts of Karst and the 3rd Appalachian Karst Symposium*, Shepherdstown, West Virginia: National Cave and Karst Research Institute, (2018). DOI: <https://doi.org/10.5038/9780991000982.1040>
- [49] M. Caudron, F. Emeriault, R. Kastner, M. Al Heib, Numerical modeling of the soil structure interaction during sinkholes. *Numerical methods in geotechnical engineering*, Graz, Austria, 267-273 (2006).
- [50] J. Zhu, A.M. Nolte, N. Jacobs, M. Ye, Using machine learning to identify karst sinkholes from LiDAR-derived topographic depressions in the Bluegrass Region of Kentucky. *Journal of Hydrology* **588**, 125049 (2020). DOI: <https://doi.org/10.1016/j.jhydrol.2020.125049>.
- [51] J. Zhu, W.P. Pierskalla, Applying a weighted random forests method to extract karst sinkholes from LiDAR data. *Journal of Hydrology* **533**, 343–352 (2016). DOI: <https://doi.org/10.1016/j.jhydrol.2015.12.012>
- [52] X. Miao, X. Qiu, S-S. Wu, J. Luo, D.R. Gouzie, H. Xie, Developing Efficient Procedures for Automated Sinkhole Extraction from Lidar DEMs. *Photogramm Eng Remote Sensing* **79**, 545-554 (2013). DOI: <https://doi.org/10.14358/PERS.79.6.545>
- [53] Y.J. Kim, B.H. Nam, Q. Zheng, An artificial neural network approach to sinkhole hazard assessment for East Central Florida. *Proceedings Of The 16th Multidisciplinary Conference On Sinkholes And The Engineering And Environmental Impacts Of Karst*, Puerto Rico: National Cave and Karst Research Institute, (2020). DOI: <https://doi.org/10.5038/9781733375313.1031>
- [54] K. Taheri, H. Shahabi, K. Chapi, A. Shirzadi, F. Gutiérrez, K. Khosravi, Sinkhole susceptibility mapping: A comparison between Bayes-based machine learning algorithms. *Land. Degrad. Dev.* **30**, 730-745 (2019). DOI: <https://doi.org/10.1002/ldr.3255>
- [55] S. Bianchini, P. Confuorto, E. Intrieri, P. Sbarra, D. Di Martire, D. Calcaterra, F. Fanti, Machine learning for sinkhole risk mapping in Guidonia-Bagni di Tivoli plain (Rome), Italy. *Geocarto International* **37**, 16687-16715 (2022). DOI: <https://doi.org/10.1080/10106049.2022.2113455>
- [56] H.A. Nefeslioglu, B. Tavus, M. Er, G. Ertugrul, A. Ozdemir, A. Kaya, S. Kocaman, Integration of an InSAR and ANN for Sinkhole Susceptibility Mapping: A Case Study from Kirikkale-Delice (Turkey). *ISPRS International Journal of Geo-Information* **10**, 119 (2021). DOI: <https://doi.org/10.3390/ijgi10030119>
- [57] O. Alrabayah, D. Caus, R.A. Watson, H.Z. Schulten, T. Weigel, L. Rüpkke, D. Al-Halbouni, Deep-Learning-Based Automatic Sinkhole Recognition: Application to the Eastern Dead Sea. *Remote Sensing* **16**, 2264 (2024). DOI: <https://doi.org/10.3390/rs16132264>
- [58] M.U. Rafique, J. Zhu, N. Jacobs, Automatic Segmentation of Sinkholes Using a Convolutional Neural Network, *Earth and Space Science* **9**, 2 (2022). DOI: <https://doi.org/10.1029/2021EA002195>
- [59] M-S. Kang, N. Kim, S.B. Im, J-J. Lee, Y-K. An, 3D GPR Image-based UcNet for Enhancing Underground Cavity Detectability, *Remote Sensing*, **11**, 2545 (2019). DOI: <https://doi.org/10.3390/rs11212545>
- [60] E.J. Lee, S.Y. Shin, B.C. Ko, C. Chang, Early sinkhole detection using a drone-based thermal camera and image processing, *Infrared Physics & Technology*, **78**, 223–232 (2016). DOI: <https://doi.org/10.1016/j.infrared.2016.08.009>.
- [61] H.N. Vu, C. Pham, N.M. Dung, S. Ro, Detecting and Tracking Sinkholes Using Multi-Level Convolutional Neural Networks and Data Association, *IEEE Access*, **8**, 132625-132641 (2020). DOI: <https://doi.org/10.1109/access.2020.3010885>